



## Vibration attenuation in a graded metamaterial rod

Fábio C. M. Oliveira, José Maria C. dos Santos

*University of Campinas, UNICAMP-FEM-DMC  
Rua Mendeleev 200, Cidade Universitária Zeferino Vaz, Campinas - SP, Brazil  
fah\_hc@hotmail.com, zema@unicamp.br*

**Abstract.** In this work, a broadband vibration attenuation approach using a graded metamaterial rod is proposed. A set of spring-mass local resonators with different spacing are attached to an elastic rod to obtain a graded metamaterial rod. Instead of a single local resonator, two or more integrated resonators are used in each unit cell. The Finite Element (FE) method and the Spectral Element (SE) method are used to model the graded metamaterial rod. A simulated study is conducted to investigate the effects of the length spacing in the graded metamaterial rod. Simulated example results in terms of attenuation constant, frequency response function (FRFs), transmittance and dispersion diagram are presented and discussed.

**Keywords:** Graded metamaterial, Phononic crystals, Stop-band, Spectral element, Finite element.

### 1 Introduction

Wave propagation through metamaterials (MMs) and phononic crystals (PCs) have attracted significant research interest in the last decades. They are man-made artificial materials, broadly investigated due to unusual properties such as negative effective mass, stiffness, and bulk modulus [1–3]. These materials can be used for vibration and noise control, acoustic cloaking, seismic shields, acoustic wave lenses, wave trapping and acoustic black holes [1]. This is due to the capacity to generate bandgaps within which no waves can propagate. However, the application has physical limitations to produce large or multiple stop-bands, one of the strategies to mitigate this limitation is through a gradation of local resonators (LR) mass, frequency or spacing leading to larger and/or multiple bandgaps [4]. A structure with a distribution of LR that can generate multi-frequency bandgaps is rainbow metamaterial [1, 5]. Periodic spring-mass LR are limited to a restrained frequency range [6]. Recently, some works presented aperiodic and periodic MMs using graded LR. Hu et al. [4] simulated an aperiodic beam with LR of the same mass and different natural frequencies coupled to the structure, the distance between the LR is constant. The gradation in natural frequencies follows an Arithmetic Progression (AP). A 172.8% increase in attenuation was observed when compared to a conventional MM. Meng et al. [7] used optimization methods to generate a rainbow MM constitutive of a  $\Pi$ -shaped beam with parallel plate insertions and two sets of spatially varying cantilever-mass resonators. Optimal beams by different optimization strategies exhibited different resonator distributions and hence various FRF properties. Banerjee [8] used a periodic gradation in the distance (GD) between two successive LRs and gradation in their mass keeping the total mass of the resonator in a unit cell unaltered. The distance spacing is an AP.

Based on this approach, a graded MM composed by a gradation in the distance between the LR attached to a host longitudinal rod is proposed in the present study. To demonstrate the rainbow effects, a conventional periodic metamaterial is investigated. New strategies such as Geometric Progression (GP) and Fibonacci Sequence (FS) are proposed and compared with arithmetic progression, conventional MM with equal spacing between LR and a rod without LR (bare rod). Rods are modeled by the Spectral Element Method (SEM) and verified by the Finite Element Method (FEM). Simulated results are compared to each other and the results showed that the periodic graded metamaterial rod with GD has extended stop-bands compared with the conventional one.

## 2 Periodic Metamaterial Modeling

### 2.1 Rod Spectral Element

The free longitudinal vibration of a uniform rod in the frequency domain can be expressed as [9]:

$$EAU'' + \omega^2 \rho AU = 0. \quad (1)$$

where  $U$  is the longitudinal displacement,  $E$  is the Young's modulus,  $A$  is the cross section area,  $\rho$  is the mass density, and  $(')$  denotes space derivatives. To include damping in the model a complex Young's modulus is used,  $E_c = E(1 + i\eta)$ , where  $\eta$  is a loss factor and  $i$  is the imaginary unity.

By assuming the general solution of Eq. (1) as  $U(x) = ae^{-ik_L x}$  and substituting in it, the dispersion relation  $k^2 - k_L^2 = 0$  is obtained, which has two roots  $k_1 = -k_2 = k_L$ , where  $k_L = \omega\sqrt{\rho/E}$  is the rod wavenumber.

A two nodes rod spectral element scheme and the internal forces is presented in Figure 1.

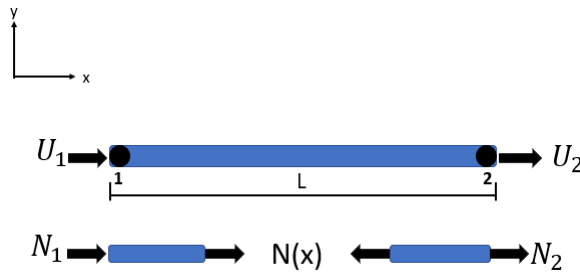


Figure 1. Two nodes rod spectral element scheme.

Considering a finite rod element of length  $L$ , the general solution to Eq. (1) can be written as:

$$U(x) = a_1 e^{-ik_L x} + a_2 e^{ik_L x} = \mathbf{B}(x)\mathbf{a} \quad (2)$$

where  $\mathbf{B}(x) = [e^{-ik_L x} \quad e^{ik_L x}]$  and  $\mathbf{a} = \{a_1 \quad a_2\}^T$ . The spectral nodal displacements can be related to the displacement field as  $\mathbf{d} = \{U_1 \quad U_2\}^T = \{U(0) \quad U(L)\}^T$ , and substituting in the Eq.(2) produces:

$$\mathbf{d} = \begin{bmatrix} B(0) \\ B(L) \end{bmatrix} \mathbf{a} = \mathbf{H}_R \mathbf{a}, \quad (3)$$

where

$$\mathbf{H}_R(\omega) = \begin{bmatrix} 1 & 1 \\ e^{-ik_L L} & e^{ik_L L} \end{bmatrix} \quad (4)$$

The spectral components of the axial force are related to  $U(x)$  by

$$N(x) = EAU'(x). \quad (5)$$

The nodal forces defined for the finite rod element (Fig. 1) can be expressed to the internal forces defined by the strength of materials as  $\mathbf{f}_c(\omega) = \{N_1 \quad N_2\}^T = \{-N(0) \quad N(L)\}^T$ , substituting into the Eq. (5) and (2), it has:

$$\mathbf{f}_c = \begin{bmatrix} -N(0) \\ N(L) \end{bmatrix} \mathbf{a} = \mathbf{M}_R \mathbf{a}, \quad (6)$$

where

$$\mathbf{M}_R(\omega) = ik_L EA \begin{bmatrix} 1 & -1 \\ -e^{-ik_L L} & e^{ik_L L} \end{bmatrix} \quad (7)$$

From the Eq. (6) and (3) a force-displacement relationship is obtained as  $\mathbf{f}_c = \mathbf{M}_R(\mathbf{H}_R)^{-1} \mathbf{d}$ , where  $\mathbf{M}_R(\mathbf{H}_R)^{-1} = \mathbf{S}_R(\omega)$  is the rod spectral element matrix given by:

$$\mathbf{S}_R(\omega) = \begin{bmatrix} S_{R11} & S_{R12} \\ S_{R21} & S_{R22} \end{bmatrix} \quad (8)$$

where  $S_{R11} = S_{R22} = (k_L EA) \cot(k_L L)$  and  $S_{R12} = S_{R21} = -(k_L EA) \csc(k_L L)$ . The transmittance of the metamaterial rod can be expressed as:

$$T(\omega) = \left| \frac{U_1(\omega)}{U_N(\omega)} \right| \quad (9)$$

where  $N$  is the number of metamaterial rod unit-cells.

## 2.2 Local Resonator

The LR is modeled by a spring ( $k_r$ ) mass ( $m_r$ ) resonator connected into the left-hand node of the rod spectral element of length ( $L_i$   $i = 1, \dots, 6$ ). The unit cell is composed by six LRs with the total length  $L_{cell} = \sum_{i=1}^6 L_i$ . Figure 2 shows the rod schemes that will be simulated. The Fig. 2(a), refers to a bare rod, i.e., a rod without LR. Figure 2(b) shows a conventional MM rod with the same mass, stiffness and equally spaced LRs. Figure 2(c) shows a MM rod with the same mass and stiffness, but with a gradation in the distance (GD) between LRs. For the GD case, three different sequences were analyzed: Arithmetic Progression (AP), Geometric Progression (GP) and Fibonacci Sequence (FS).

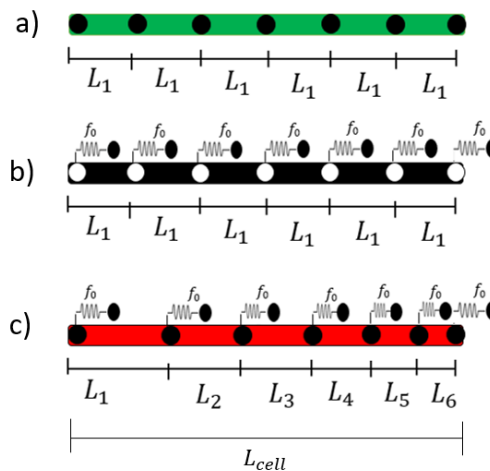


Figure 2. Metamaterial rod unit-cell scheme a) Bare Rod (BR); b) Constant Distance (CD); and c) Graded Distance (GD).

From the reference [2] the spring-mass dynamic stiffness at the attachment point of the rod spectral element can be expressed as  $S_0 = k_r - k_r(k_r - \omega^2 m_r)^{-1} k_r$ , where  $m_r$  and  $k_r$  are mass and stiffness of the spring-mass system, respectively. By coupling the spring-mass system at the left-hand side node of the rod spectral element the LR dynamic stiffness matrix is obtained as:

$$\mathbf{S}_{LR}(\omega) = \begin{bmatrix} S_{R11} + S_0 & S_{R12} \\ S_{R21} & S_{R22} \end{bmatrix} \quad (10)$$

### 3 Simulated Results

Table 1 presents the geometry and material properties used for all simulated examples. The gradation distance parameter in AP and GP is  $L_1$ , which is the distance between the first and second LR, and  $R$  is the progression ratio. For FS,  $L_6$  and  $L_5$  are the gradation distance parameter.

Table 1. Simulated metamaterial rod geometry and material property.

Geometry/Property	Value
Unit-cell length ( $L_{cell}$ )	2.6718 m
Cross section area ( $A$ )	$1.13 \times 10^{-4} \text{ m}^2$
Number of unit-cells ( $N$ )	6
Young's modulus ( $E$ )	15 GPa
Mass density ( $\rho$ )	1200 kg/m <sup>3</sup>
Structural damping ( $\nu$ )	0.01
LR masses ( $m_0$ )	0.02 kg
AP gradation	$L_1 = 0.89\text{m} / R_{AP} = -0.18$
GP gradation	$L_1 = 1.72\text{m} / R_{GP} = 0.35$
FS series	$L_i = \{1.06, 0.66, 0.40, 0.26, 0.13, 0.13\}$

Figure 3 shows the Frequency Response Function (FRF) at the transfer and drive points, and the Transmittance calculated by SEM and FEM methods for a periodic rod, with free-free (F-F) boundary conditions and six equally spaced unit cells with one LR coupled. For the SEM one spectral element is used for each length between LRs, while the FEM method used 25 elements between LRs. The FRFs and Transmittance results present a good agreement between the methods. The bandgap visualized in the FRFs are corroborated by the transmittance attenuation. From the FRFs it can be seen the metamaterial rod first natural frequency at 330 Hz, for this reason, in the next simulations will use LR with a natural frequency of 300 Hz.

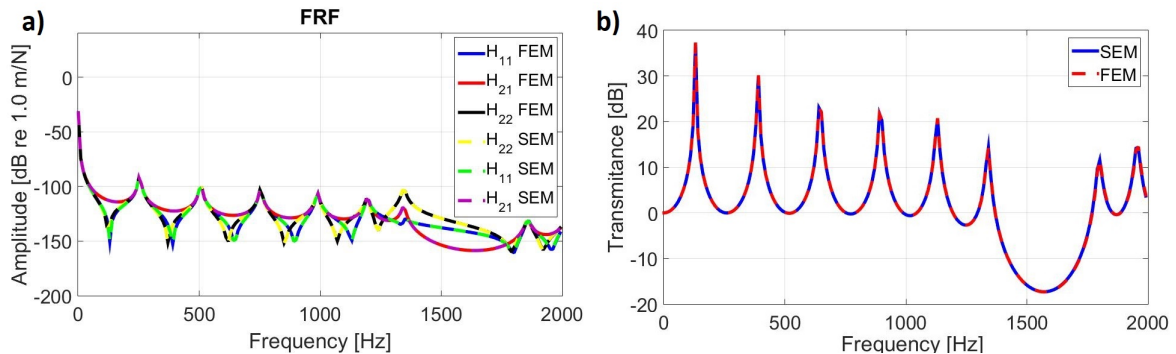


Figure 3. Metamaterial rod calculated by SEM and FEM: a) Frequency Response functions and b) Transmittance.

From now on, all the simulated examples will be calculated only by SEM. Three simulated examples are performed using metamaterial rod with unit-cell gradation in the distance (GD) between two successive LR using arithmetic progression (AP), geometric progression (GP) and Fibonacci series (FS). Dispersion diagram and Transmittance are calculated for a metamaterial GD generated by AP, GP and FS, and the results are compared with that obtained with a bare rod (BR) and a metamaterial rod with unit-cell constant in the distance (GD) between successive LR (Fig. 4). The Fig. 4(a) shows the dispersion diagram (*left plot*) and transmittance (*right plot*) for

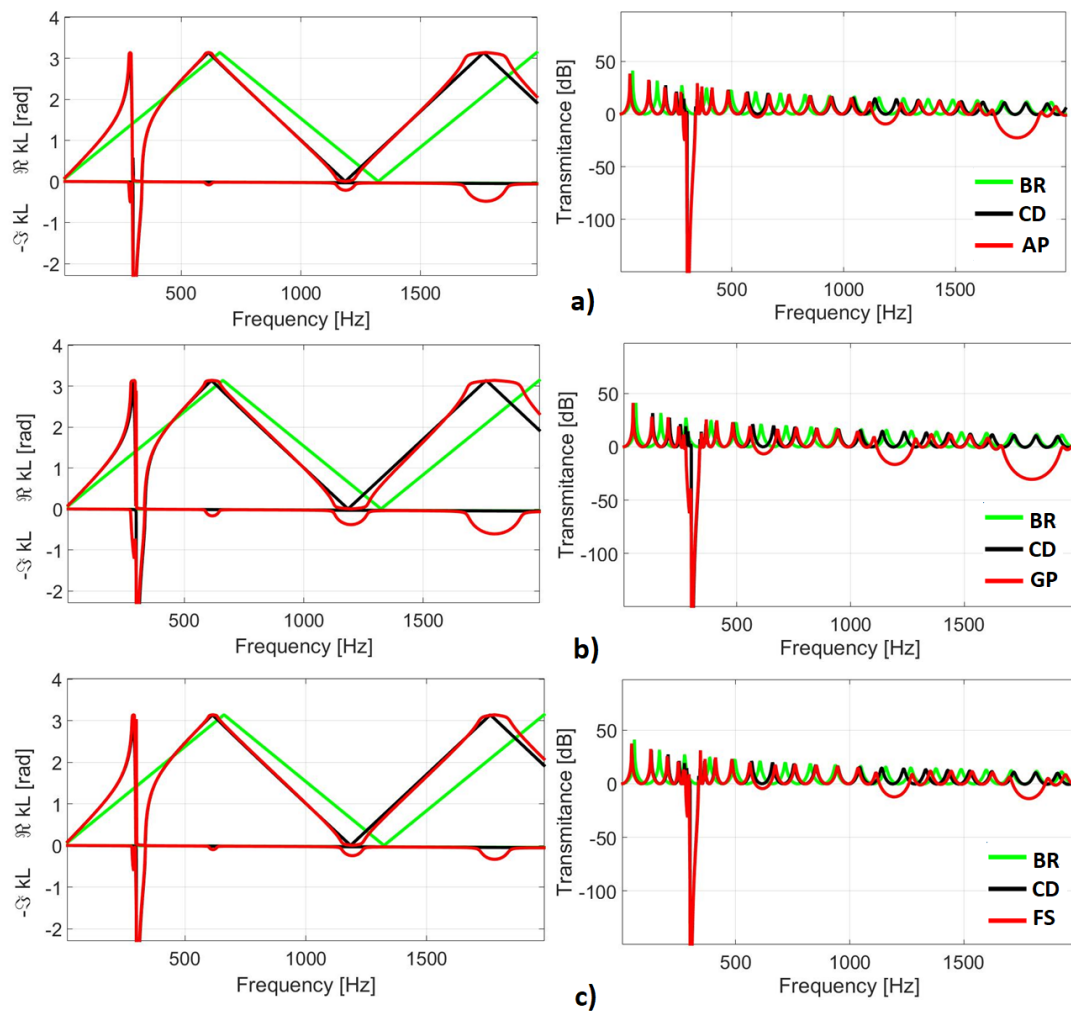


Figure 4. Dispersion diagram (*left*) and Transmittance (*right*) for a Bare Rod (BR) and metamaterial rod with Constant Distance (CD) between LR compared with metamaterial rods with: a) Arithmetic Progression (AP), b) Geometric Progression (GP) and c) Fibonacci Series (FS) distance between LR.

a metamaterial rod with a GD generated by AP, and compared to BR and CD. At the local resonance frequency (300 Hz) a same width bandgap appears for the AP and CD cases, while at higher frequencies there is three larger Bragg-type bandgaps AP case. Figure 4(b) shows the dispersion diagram (*left plot*) and transmittance (*right plot*) for a metamaterial rod with a GD generated by GP, and compared to BR and CD. It is noticed a widening of the LR bandgap and the attenuation level is started at a lower frequency as compared to that of CD. Bragg-type bandgaps occur in frequency bands similar to those found in AP case, but with larger bandgap width and attenuation level. Figure 4(c) shows the dispersion diagram (*left plot*) and transmittance (*right plot*) for a metamaterial rod with a GD generated by FS, and compared to BR and CD. It can be seen that the LR type bandgap are similar to that obtained in CD case, but at the frequencies where the Bragg-type bandgaps occur, also attenuation level increases as compared to CD case. For all analysed cases the BR was kipped in order to emphasizing the transmittance attenuation level obtained by metamaterials rods.

Figure 5 shows a comparison of the dispersion diagram and transmittance results between CDs generated by AP, GP and FS. From the dispersion diagram (Fig. 5(a)) It can be seen that the metamaterial rod using GD with

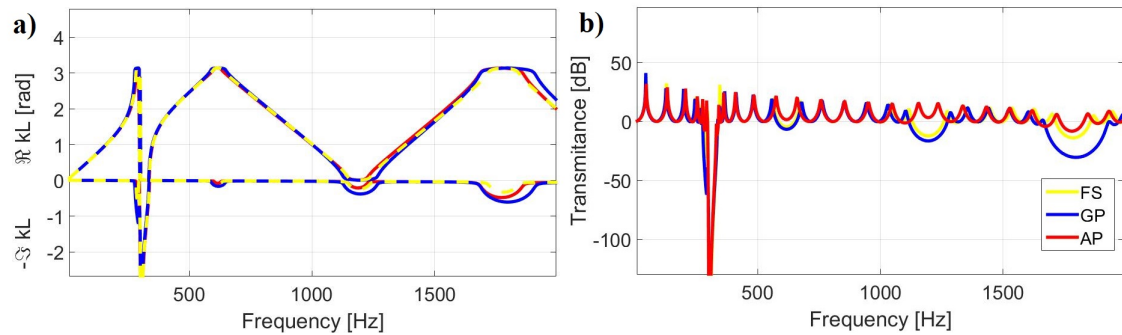


Figure 5. Comparison between metamaterial rod using GD with AP, GP and FS: a) Dispersion diagram and b) Transmittance.

GP present the larger bandgap width followed by GD with AP and FS. This results indicates tha GD with GP are more effective into produce larger bandgaps the the other approaches. Similar behavior should be noticed in the transmittance results (Fig. 5(a)), but it does not happens. Although the rod metamaterial bandgaps generated by GD with GP and FS presents an attenuation level in good correlation with the dispersion results, the rod metamaterial bandgap generated by GD with AP does not present the same results.

## 4 Conclusions

In this study, a periodic metamaterial rod with gradation in the distance (GD) between two subsequent spring mass resonator was presented and modeled by the Spectral Element Method (SEM). The simulated results of GD are compared to a bare rod (BR) and a metamaterial with constant distance (CD) between subsequent LR using the dispersion diagram and transmittance. In structures where vibration attenuation with weight limitation is required, the use of GD is a good alternative Three types of GD were simulated and compared: Arithmetic Progression (AP), Geometric Progression (GP) and Fibonacci Sequence (FS). Bandgaps GP showed greater attenuation as compared with AP and FS. In the next steps methods of optimization will be used for determine the GD best parameters. Also the frequency and mass gradation will be explored, evaluated and combine with the GD.

**Acknowledgements.** The authors are thankful to CAPES (Finance Code 001), FAPESP (Grant No. 2018/15894-0), and CNPq (Grant No. 313620/2018) for the financial support. .

**Authorship statement.** The authors hereby confirm that they are the sole liable persons responsible for the authorship of this work, and that all material that has been herein included as part of the present paper is either the property (and authorship) of the authors, or has the permission of the owners to be included here.

## References

- [1] H. Meng, D. Chronopoulos, and A. T. Fabro. A rainbow metamaterial for broadband multi-frequency vibration suppression. *INTER-NOISE 2019 MADRID - 48th International Congress and Exhibition on Noise Control Engineering*, vol. 163, 2019.
- [2] E. D. Nobrega, F. Gautier, A. Pelat, and J. M. Dos Santos. Vibration band gaps for elastic metamaterial rods using wave finite element method. *Mechanical Systems and Signal Processing*, vol. 79, pp. 192–202, 2016.
- [3] A. Banerjee, R. Das, and E. P. Calius. Frequency graded 1D metamaterials: A study on the attenuation bands. *Journal of Applied Physics*, vol. 122, n. 7, 2017.
- [4] G. Hu, A. C. M. Austin, V. Sorokin, and L. Tang. Metamaterial beam with graded local resonators for broadband vibration suppression. *Mechanical Systems and Signal Processing*, vol. 146, pp. 106982, 2021.
- [5] J. Zhu, Y. Chen, X. Zhu, F. J. Garcia-Vidal, X. Yin, W. Zhang, and X. Zhang. Acoustic rainbow trapping. *Scientific Reports*, vol. 3, n. medium I, pp. 1–6, 2013.
- [6] E. Miranda Jr. and J. M. Dos Santos. Flexural wave band gaps in multi-resonator elastic metamaterial Timoshenko beams. *Wave Motion*, vol. 91, pp. 102391, 2019.

- [7] H. Meng, N. Bailey, Y. Chen, L. Wang, F. Ciampa, A. Fabro, D. Chronopoulos, and W. Elmadih. 3D rainbow phononic crystals for extended vibration attenuation bands. *Scientific Reports*, vol. 10, n. 1, pp. 1–9, 2020.
- [8] A. Banerjee. Flexural waves in graded metabeam lattice. *Physics Letters, Section A: General, Atomic and Solid State Physics*, vol. 388, pp. 127057, 2021.
- [9] U. Lee. *Spectral Element Method in Structural Dynamics*, 2009.